Original article

LuoFuShan Rheumatism Plaster ameliorates neuropathic pain in mice by suppressing TLR4/TNF-α signaling

FU Yufang[1], TAN Weiling[1,2], LI Xiaocui[1], LIN Rongtian[3], LIU Shuwen[1,4,5], YE Ling[1,5]

[1]School of Pharmaceutical Sciences, [2]School of Traditional Chinese Medicine, Southern Medical University, Guangzhou 510515, China; [3]Guangdong Engineering Research Center for Anti-Rheumatic Traditional Chinese Medicine, R&D Center, Guangdong Luofushan Sinopharm Co., Ltd., Huizhou 516100, China; [4]Department of Pharmacy, Pingshan Hospital, Southern Medical University, Shenzhen 518100, China; [5]Guangdong Basic Research Center of Excellence for Integrated Traditional and Western Medicine for Qingzhi Diseases, Guangzhou 510515, China

Abstract: Objective To explore the therapeutic effect of *LuoFuShan* Rheumatism Plaster (LFS) on neuropathic pain (NP) and its molecular mechanism. **Methods** Mouse models of sciatic nerve chronic constriction injury (CCI) were treated with low, medium, and high doses (2.2, 4.4, and 8.8 cm^2, respectively) of LFS by topical application for 14 consecutive days. The therapeutic effects were assessed by evaluating the mechanical withdrawal threshold (MWT), paw withdrawal latency (PWL), plasma IL-6 and TNF-α levels, and histopathology of the sciatic nerve. Network pharmacology and molecular docking were used to identify the key targets and signaling pathways. The key targets were verified by RT-qPCR and immunohistochemistry. The biosafety of LFS was evaluated by measuring the organ indices and damage indicators of the heart, liver, and kidneys. **Results** Compared with the CCI group, LFS dose-dependently increased MWT and PWL, reduced plasma IL-6 and TNF-α levels, and alleviated sciatic nerve inflammation in the mouse models. Network pharmacology identified 378 bioactive compounds targeting 279 NP-associated genes enriched in TLR and TNF signaling. Molecular docking showed that quercetin and ursolic acid in LFS could stably bind to TLR4 and TNF-α. In the mouse models of sciatic nerve CCI, LFS significantly downregulated the mRNA expression levels of *Tlr4* and *Tnf-α* in the spinal cord in a dose-dependent manner and lowered the protein expressions of TLR4 and TNF-α in the sciatic nerve. LFS treatment did not cause significant changes in the organ indices or damage indicators of the heart, liver and kidneys as compared with those in the CCI model group and sham-operated group. **Conclusion** LFS alleviates NP in mice by suppression of TLR4/TNF-α-mediated neuroinflammation with a good safety profile.

Keywords: *LuoFuShan* Rheumatism Plaster; neuropathic pain; TLR4/TNF-α signaling; Safety evaluation

INTRODUCTION

Neuropathic pain (NP), a debilitating condition arising from lesions or diseases affecting the somatosensory nervous system, manifests through heterogeneous etiologies including diabetic neuropathy, chemotherapy-induced neuropathy, postherpetic neuralgia, and postsurgical nerve injury. Global epidemiological studies estimate that NP affects approximately 26 million individuals worldwide, with over 10 million cases in the United States alone, imposing a substantial economic burden exceeding $600 billion annually in direct healthcare expenditures and productivity losses[1,2]. The clinical management of NP remains particularly challenging, largely due to its pathophysiological complexity involving distinct peripheral and central sensitization mechanisms. Currently available oral agents, including serotonin-norepinephrine reuptake inhibitors, gabapentinoids, and topical nonsteroidal anti-inflammatory drugs, produce suboptimal therapeutic outcomes with delayed onset of action, systemic adverse effects (e. g., dizziness, sedation), and risks of pharmacological dependence[3,4]. In addition, even if opioid analgesics can provide transient symptomatic relief, their long-term use is severely limited by tolerance development, respiratory depression, and misuse potential that exacerbates the ongoing opioid crisis[5,6]. Recent advancements in localized drug delivery systems, particularly transdermal patches, present a promising paradigm for NP management[7]. Mechanistically, these systems enable targeted modulation of peripheral nociceptors while minimizing systemic exposure, thereby achieving therapeutic precision.

LuoFuShan Rheumatism Plaster (LFS), a black herbal patch comprising 41 traditional Chinese medicines (TCMs), has emerged as a promising transdermal therapeutic agent for NP management. Among its core TCM components, Bungarus parvus

Received: 2025-08-03 **Accepted:** 2025-09-30

Supported by Scientific Connotation of Efficacy of LuoFuShan Rheumatism Plaster Based on Clinical Orientation (K924319081); National Natural Science Foundation of China (82422077) and Natural Science Foundation of Guangdong Province (2024B1515020093).

Corresponding authors: YE Ling, PhD, professor, E-mail: yeling@smu. edu. cn; LIU Shuwen, PhD, professor, E-mail: liusw@smu.edu.cn; LIN Rongtian, E-mail: 47415242@qq.com.

exhibits validated anti-inflammatory and analgesic properties through acetylcholinesterase inhibition, while Clematis chinensis Osbeck modulates TRPV1 channels to alleviate neuropathic hyperalgesia[8, 9]. The formula integrates synergistic herbs such as *Angelica sinensis* for immunomodulation and *Panax notoginseng* for microcirculation improvement, collectively supporting its clinical outcomes, as evidenced by a 92.5% total effectiveness rate in sciatica patients[10-12]. The clinical success of LFS is further supported by its commercial profile, with annual sales exceeding RMB 112 million from 2021 to 2023. Despite these empirical and commercial successes, the pharmacological mechanisms underlying the efficacy of LFS for NP treatment remain poorly characterized.

In the current study, we systematically investigated the therapeutic potential and mechanisms of LFS for NP treatment in a mouse model of chronic constriction injury (CCI) of the sciatic nerve, and used network pharmacology and molecular docking for predicting the potential candidate targets, which were verified in the mouse models. We also assessed the biosafety of LFS for NP treatment. Our findings suggest that LFS alleviates CCI-induced NP by suppressing TLR4/TNF-α-mediated neuroinflammation with a good biosafety profile in mice.

METHODS

Chemicals and reagents

LFS (batch number L23C131) was provided by Guangdong LuoFuShan National Medicine Co., Ltd. Diclofenac sodium patch (DSP) (batch number H20051966) was purchased from Bengbu Fengyuan Tushan Pharmaceutical Co., Ltd. Commercial ELISA kits for IL-6 (m1098430) and TNF-α (m1002095) were obtained from Shanghai Enzyme-linked Biotechnology Co. (Shanghai, China). TLR4 and TNF-α antibodies were purchased from Proteintech Group, Inc. (Wuhan, China).

Animals

Male Kunming mice, aged 6-7 weeks, were obtained from Guangzhou Ruige Biotechnology Co., Ltd (Guangzhou, China) (License number: SCXK(Y)2023-0059). The mice were maintained under specific pathogen-free (SPF) conditions at the density of 5 mice per cage with controlled temperature (24±1 ℃) and humidity (55±5%) on a 12-h light/dark cycle. All the animal experimental procedures were conducted in accordance with the Guidance for the Care of Laboratory Animals and approved by the Ethics Committee of Southern Medical University (Guangzhou, China).

NP modeling

An NP model was established in mice by inducing chronic compression injury (CCI) of the sciatic nerve using a modified method from a previous study[13]. Briefly, following anesthesia induction with intraperitoneal sodium pentobarbital (2%, 50 mg/kg), the mice were fixed in a prone position and the right sciatic nerve was surgically exposed by blunt dissection. Under a microscope, 4 loosely constricting ligatures (4-0 silk sutures) were placed at 1 mm intervals along the proximal third of the nerve trunk, with subsequent closure of muscle layers and skin. The sham-operated mice underwent identical surgical procedures without nerve ligation.

Animal grouping and treatment

Forty NP model mice were selected and randomly allocated into 5 treatment groups (n=8/group), includingCCI model group (with blank patch treatment), diclofenac sodium patch (DSP; 2.5 cm^2/back) positive control group, low-dose LFS (2.2 cm^2/back, LFSL) group, medium-dose LFS (4.4 cm^2/back, LFSM) group, and high-dose LFS (8.8 cm^2/back, LFSH) group, with another 8 mice receiving the sham operation as the sham-operated group. All the interventions were administered *via* application of transdermal patches to the dorsal region for 14 consecutive days (starting on postoperative day 3), and the patches were replaced once daily. At the end of the experiment, blood samples were collected from the orbital venous plexus, and the sciatic nerve, heart, liver, and kidneys of the mice were dissected immediately.

Mechanical withdrawal threshold test

Mechanical withdrawal threshold (MWT) was quantified using von Frey filaments. The measurements of the paw withdrawal threshold were conducted on days -1, 3, 5, 9, 12, and 16. Each mouse was transferred to a standardized testing apparatus with a 5×5 mm perforated metal grid floor enclosed by a transparent acrylic chamber. The mice were acclimated to the environment for 15 min until exploratory behaviors (e. g., rearing, sniffing) ceased, and the mice were in a quiescent state. Mechanical stimuli were applied perpendicularly to the plantar surface of the hind paw using ascending-force von Frey filaments (0.4-2.0 g range) according to the up-down method[14].

Paw withdrawal thermal latency test

The paw withdrawal latency (PWL) test was conducted on days -1, 3, 5, 9, 12, and 16 using an intelligent hot plate apparatus. Specifically, the mice were individually habituated in transparent glass chambers for 15 min to minimize stress-induced behavioral variability. Thermal stimulation was delivered to the plantar surface of the hind paw using an intelligent hot plate apparatus (53 ℃) according to a previously described method[15]. The time interval between heat application and observable nocifensive behaviors (paw withdrawal or licking) was

defined as PWL. To prevent tissue damage, a safety cutoff latency of 60 s was enforced, with trials automatically terminated upon reaching this threshold.

Enzyme-linked immunosorbent assay (ELISA)

The collected blood samples were centrifuged at 4 ℃ at 3000 r/min for 10 min for plasma separation. The isolated plasma was used to quantify IL-6 and TNF-α levels following the standardized protocol provided by the ELISA kits (Shanghai Enzyme-linked Biotechnology Co., Ltd., Shanghai, China).

Hematoxylin-eosin (HE) staining

The harvested nerve specimens were fixed in 4% neutral buffered paraformaldehyde for 48 h, paraffin-embedded and sectioned at 3 μm thickness. Deparaffinization was performed through sequential xylene immersion (2× 5 min), followed by rehydration in descending ethanol gradients. For histopathological evaluation, the sections were stained using a commercial HE kit (Beyotime, China) according to standardized protocols. Images of all the nerve specimens were captured using an upright microscope (Nikon, Japan). A semi-quantitative scoring system was used to evaluate myelin degeneration, inflammation, and Schwann cell proliferation in HE-stained sections[16].

Network pharmacology analysis

Through the Traditional Chinese Medicine Systematic Pharmacology Database and Analysis Platform (TCMSP, http://tcmspw. com/tcmsp. php), the relevant chemical constituents and targets of LFS were searched. Meanwhile, the information of targets related NP was searched in GeneCards database (https://www.genecards. org/) and OMIM database (https://www. omim. org/). The protein-protein interaction (PPI) network of the intersection targets between LFS and NP was constructed from the STRING (https://string-db. org/). The hub genes were identified and visually analyzed using Cytoscape software. The common targets were submitted into Metascape (https://metascape. org/) for Gene Ontology (GO) function and Kyoto Encyclopedia of Genes and Genomes (KEGG) pathway enrichment analyses[17].

Molecular docking analysis

The 3D structures of quercetin (PubChem CID: 5280343) and ursolic acid (PubChem CID: 64945) were retrieved in SDF format from the PubChem database. The 3D crystal structures of TLR4 (PDB ID: 2Z63) and TNF-α (PDB ID: 1A8M) were downloaded from the Protein Data Bank (PDB) (https://www. rcsb. org/). Molecular docking was then performed using AutoDock Vina. The top-ranked binding poses were visualized and analyzed using PyMOL 2.5.4.

Quantitative reverse transcription-polymerase chain reaction (RT-qPCR)

Total RNA was extracted from frozen spinal cord tissues using the Animal Total RNA Isolation Kit (FOREGENE, Chengdu, China). cDNA was synthesized with the Color Reverse Transcription Kit (A0010C, EZBioscience, Roseville, CA, USA). RT-qPCR was performed using the SYBR Green/Rox qPCR master Mix (A0010C, EZBioscience, Roseville, CA, USA) according to the manufacturer′s instruction. The expression levels of the target genes were normalized to the reference gene *Gapdh* and the fold changes were calculated using the $2^{-\Delta\Delta CT}$ method. All the primers were synthesized by Tsingke Biotechnology Co., Ltd. (Beijing, China). The primer sequences are listed below:

Gapdh, 5'-AGGTCGGTGTGAACGGATTTG-3' (F),
5'-TGTAGACCATGTAGTTGAGGTCA-3' (R);
Tlr4, 5'-ATTACCCGCCCGAGAAAGG-3' (F),
5'-TCGCAGCAAAGATCCACACAG-3′ (R);
Tnf-α, 5'-CCTGTAGCCCACGTCGTAG-3' (F),
5'-GGGAGTAGACAAGGTACAACCC-3' (R).

Immunohistochemical (IHC) analysis

The protein expressions of TLR4 and TNF-α in the sciatic nerve tissues were detected using IHC. Briefly, the sciatic nerve tissues from 3 mice per group were fixed in 4% neutral buffered paraformaldehyde for 48 h and sectioned at 3 μm thickness. After blocking with 3% bovine serum albumin solution for 30 min, the sections were treated in sodium citrate antigen repair solution (1∶1000 dilution, pH 6.0), and incubated overnight at 4 ℃ with the primary antibodies, namely rabbit anti-TLR4 monoclonal antibody (1∶500, 66350-1-Ig, Proteintech) and rabbit anti-TNF-α polyclonal antibody (1∶500; HYP80914, MedChemExpress). Following PBS-T (0.05% Tween 20) washes, the sections were treated with HRP-conjugated goat anti-rabbit IgG secondary antibody (1∶500 dilution, LF101, Yaenzyme) for 2 h at room temperature, washed with 0.1 mol/L PBS, and then incubated with DAB substrate for color development. The sections were then cleared, dehydrated, and xylene-sealed after washing with distilled water. An Olympus fluorescence microscope (BX53) was used to capture the images. The mean OD was analyzed using Image-Pro Plus 6.0 (Media Cybernetics, Inc., Rockville, MD, USA).

Biosafety assessment of LFS

To evaluate the biosafety profile of LFS during NP intervention, multi-organ toxicity indices were determined. The organ indices of the heart, liver, and kidneys of the mice were calculated using the following equation:

$$\text{Organ index}(\%) = \frac{\text{Organ wet weight}(\text{mg})}{\text{Body weight}(\text{g})} \times 100\%$$

Meanwhile, the tissues damage indicators, the lactate dehydrogenase (LDH, A020-2-2) and creatine

kinase (CK, A032-1-1) for the heart, the aspartate aminotransferase (AST, C010-2-1) and alanine aminotransferase (ALT, C009-2-1) for the liver, blood urea nitrogen (BUN, C013-2-1) and serum creatinine (Scr, C011-2-1) for the kidneys were determined using commercial kits (Nanjing Jiancheng Bioengineering Institute, Nanjing, China).

Statistical analysis

Data analysis and plotting were performed using GraphPad Prism 9.5.1 software (San Diego, California, USA). Statistical tests were selected based on appropriate assumptions with respect to data distribution and variance characteristics. The significance between two groups was evaluated using two-sided unpaired Student's *t*-test (parametric) or unpaired Mann-Whitney test (nonparametric). Comparisons among multiple groups were made using one-way analysis of variance (ANOVA) with Tukey's or Dunnett's post hoc test (parametric) or Kruskal-Wallis *H* test with Dunn's multiple comparisons test (nonparametric). A *P* value less than 0.05 was considered to indicate a statistically significant difference.

RESULTS

LFS ameliorates CCI-induced NP in mice

To investigate the effects of LFS on CCI-induced NP, the mice were treated with low, medium and high doses of LFS for 14 consecutive days (Fig. 1A). Behavioral assessments with von Frey filaments and hot-plate pain test (Fig. 1B) revealed significant mechanical and thermal hypersensitivity in CCI mice relative to the sham-operated mice ($P<0.05$; Fig. 1C and D). LFS treatment dose-dependently ameliorated these nociceptive behaviors, and high-dose LFS restored the mechanical thresholds from 0.58 to 1.34 and the thermal thresholds from 4.76 to 9.13 (Fig. 1C and D). LFS treatment also effectively reduced the secretion of IL-6 and TNF-α in a dose-dependent manner ($P<0.05$; Fig. 1E and 1F). Histopathological analysis further demonstrated that LFS treatment significantly attenuated sciatic nerve demyelination and improved nerve fiber compactness ($P<0.05$; Fig. 1G). These findings indicate that LFS mitigates NP through mechanisms that produce anti-inflammatory and neuroprotective effects.

Network pharmacology reveals multi-target mechanisms of LFS against NP

Tab. 1 summarizes the identification of 378 potential active components in LFS, derived from the TCMSP database and screened using a drug-likeness (DL>0.18). Target mapping identified 279 NP-associated targets (Fig. 2A). These potential targets were used construct PPI network using STRING database (Fig. 2B). PPI network analysis highlighted TNF, STAT3, and MARK1 as the hub nodes, and the compound-target-disease network implicated inflammatory pathways (Fig. 2C and 2D), which were supported by GO enrichment showing cytokine-mediated signaling and receptor complex activity (Fig. 2E). KEGG analysis further prioritized Toll-like receptor (TLR) and TNF signaling as key pathways (Fig. 2F).

Molecular docking validates TLR4/TNF-α interactions with LFS components

TLR4 and TNF-α are identified as the pivotal proteins involved in the TLR and TNF signaling pathways, respectively. The targets of the active ingredients of LFS were retrieved from the TCMSP database, the data were then imported into Cytoscape software for subsequent analysis, and the results are shown in Tab.2. To further investigate the roles of these two proteins in the anti-NP effects of LFS, we carried out molecular docking analysis focusing on the top two bioactive components quercetin and ursolic acid (Tab. 2). For quercetin, the calculated binding free energy (ΔG) values were -6.9 kcal/mol for TLR4 and -7.1 kcal/mol for TNF-α, indicating a favorable binding affinity. As depicted in Fig. 3A and 3B, quercetin formed hydrogen bonds with Thr399 of TLR4 at a bond length of 2.1 Å and with Tyr151 of TNF-α at a bond length of 1.9 Å, which contributed to the stabilization of the ligand-receptor complexes. Regarding ursolic acid, it exhibited a relatively high affinity for both targets, with ΔG values of -6.3 kcal/mol for TLR4 and -7.3 kcal/mol for TNF-α. As shown in Fig. 3C and 3D, ursolic acid interacted with Leu387 of TLR4 and Phe124 of TNF-α *via* hydrophobic interactions, which might be the major driving force for its binding. These molecular docking results suggest that quercetin and ursolic acid can stably bind to TLR4 and TNF-α, potentially modulating the TLR4/TNF-α signaling pathways, which may contribute to the anti-NP effects of LFS.

LFS suppresses TLR4/TNF-α signaling in the spinal cord and sciatic nerve

We further conducted RT-qPCR and IHC analysis to confirm the roles of TLR4/TNF-α signaling in alleviating NP by LFS. Our results demonstrated that LFS significantly down-regulated the relative mRNA levels of *Tlr4* and *Tnf-α* in the spinal cord in a dose-dependent manner when compared to the CCI model group ($P<0.05$; Fig. 4A and 4B). IHC staining confirmed that the expressions of TLR4 and TNF-α proteins in the sciatic nerve were also reduced ($P<0.05$; Fig. 4C and 4D). These results align with network pharmacology predictions and molecular docking fitting.

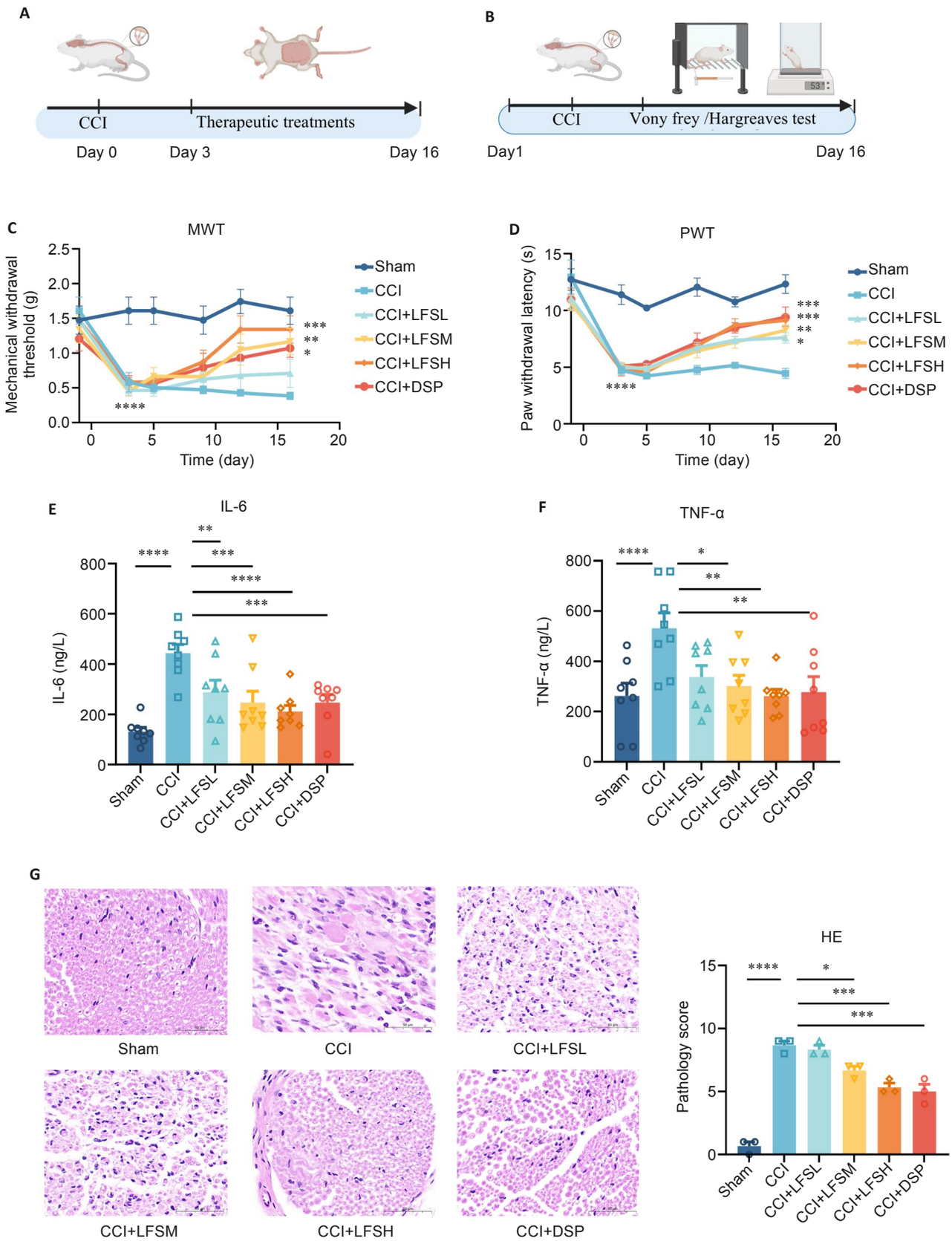

Fig. 1 LFS ameliorates CCI-induced NP in mice. **A**: Schematic illustration of the experimental design. **B**: Timeline of measuring mechanical pain threshold and thermal pain threshold in mice. **C, D**: Results of mechanical withdrawal threshold test and paw withdrawal latency test (n=8). **E, F**: Levels of IL-6 and TNF-α in plasma (n=8). **G**: HE staining of the sciatic nerve and histological scores (Original magnification: ×100, n=3). LFSL: Low-dose (2.2 cm^2/back) LFS group; LFSM: Medium-dose (4.4 cm^2/back) LFS group; LFSH: High-dose (8.8 cm^2/back) group. Data are presented as *Mean±SE*. **P*<0.05, ***P*<0.01, ****P*<0.001, *****P*<0.0001.

Tab.1 Key chemical components of LFS in treating NP

Name of Chinese medicine	Quantity of active ingredients
Angelica sinensis	67
Zanthoxylum nitidum	22
Drynaria fortunei	20
Carthamus tinctorius	18
Rubia cordifolia	17
Litsea cubeba	17
Saposhnikovia divaricata	15
Leonurus japonicus	14
Ephedra sinica	11
Datura metel	10
Stephania tetrandra	9
Achyranthes bidentata	8
Notopterygium incisum	7
Dictamnus dasycarpus	6
Aconitum kusnezoffii	6
oxicodendron vernicifluum	6
Angelica pubescens	5
Entada phaseoloides	5
Viscum coloratum	5
Schizonepeta tenuifolia	5
Strophanthus divaricatus	5
Eleutherococcus gracilistylus	5
Abrus cantoniensis	4
Dipsacus asperoides	4
Panax notoginseng	3
Aconitum carmichaelii	2
Erycibe obtusifolia	2
Bungarus multicinctus	2
Laggera alata	2
Chaenomeles speciosa	2
Schefflera arboricola	2
Pseudolarix amabilis	2
Semiliquidambar cathayensis	1
Ricinus communis	1
Dioscorea hypoglauca	1
Tinospora sinensis	1
Adenosma glutinosum	1
Clematis chinensis	1
Ardisia crenata	1
Cynanchum paniculatum	1
Pinus tabuliformis	1
Component shared by multiple drugs	61
Total	378

Biosafety evaluation of LFS

We also investigated the biosafety of LFS for NP treatment by assessing the organ indices and corresponding damage indicators for the heart, liver and kidneys. As shown in Fig.5A-C, no changes in the organ indices of the heart, liver, and kidneys were observed in the NP models after 14 days of LFS treatment at all the 3 doses LFS. No significant differences were found in plasma levels of heart damage indicators (LDH and CK), liver injury indicators (AST and ALT), or kidney damage indicators (BUN and Scr) between the mouse models after 14 days of LFS treatment and those in the CCI model and sham operation groups (P>0.05; Fig. 5D-I). Collectively, these results strongly support the biological safety of LFS in the treatment of NP.

DISCUSSION

This study provides the first comprehensive evidence that LFS, a multi-herbal transdermal formulation, effectively alleviates NP in a CCI mouse model. Our data demonstrate that LFS exerts dose-dependent anti-nociceptive effects by suppressing TLR4/TNF-α -mediated neuroinflammation while maintaining an excellent biosafety profile. These findings not only validate the clinical use of LFS but also offer a mechanistic framework for the development of transdermal herbal therapies for NP.

The management of NP remains challenging due to its multifactorial pathogenesis involving molecular dysfunction, neuroinflammation, and behavioral abnormalities[1]. With its 41 bioactive components, LFS exerts multi-action therapeutic effects against NP through synergistic inhibition of peripheral sensitization (mainly achieved by *Zanthoxylum nitidum* and *Aconitum carmichaelii*), attenuation of neuroinflammation (mainly achieved by *Angelica sinensis*, *Panax notoginseng* and *Rubia cordifolia*), and improvement of microcirculation (mainly achieved by *Leonurus japonicus*)[18-23]. Our data also supported its efficacy for NP treatment, and demonstrated its dose-dependent effects for restoring the mechanical and thermal thresholds, suppressing pro-inflammatory cytokines IL-6 and TNF-α, and improving histopathological changes in sciatic nerve demyelination, suggesting the adaptability of LFS for addressing heterogeneous NP etiologies. Crucially, the transdermal delivery system maintains a favorable biosafety profile without significant adverse effects on the heart, liver or kidneys or on tissue damage biomarkers (LDH/CK, AST/ALT, and BUN/Scr), underscoring its advantages over the conventional oral medications that have the risks of opioid-induced hyperalgesia and tricyclic antidepressant-related anticholinergic effects[5,6]. These attributes position LFS as a viable therapeutic alternative for vulnerable populations, particularly those with hepatic/renal comorbidities contraindicated for systemic pharmaco-

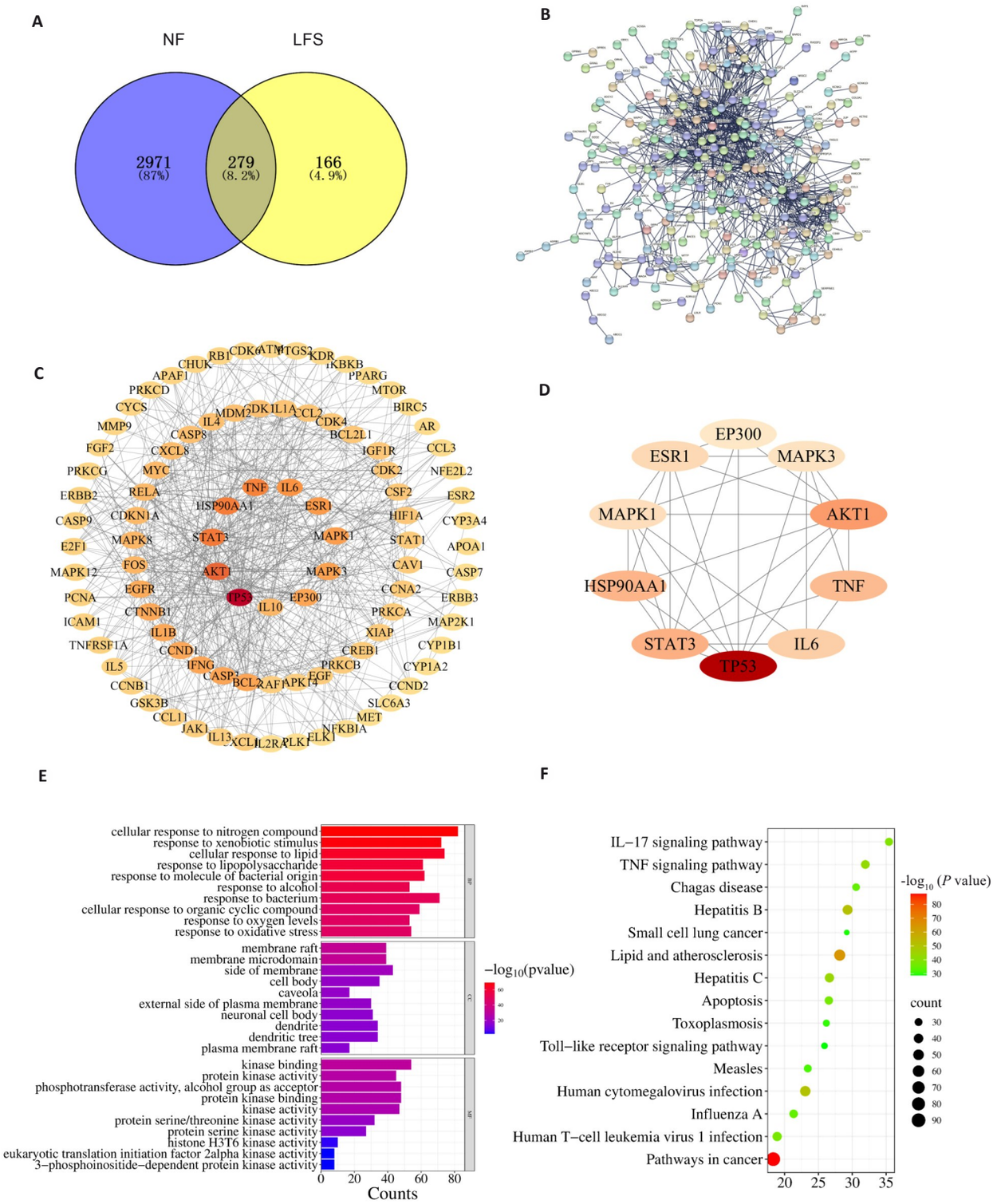

Fig. 2 Network pharmacology reveals multi-target mechanisms of LFS against NP. **A**: Diagram of Venn analysis of the intersection targets between LFS and NP. **B**: PPI network of the targets regulated by LFS. **C, D**: PPI network of NP and LFS intersection targets and key targets. **E, F:** GO functional enrichment analysis and KEGG pathway analysis of LFS in the treatment of NP.

therapies.

In the NP pathological process, TLR4-medicated neuroinflammation is confirmed as the core mechanism driving peripheral and central sensitization[24, 25]. Activation of spinal microglial TLR4 exacerbates cytokine production (e. g., IL-6) and promotes mechanical/thermal hypersensitivity following nerve injury[25]. In addition, approaches that interfere with TNF-α signaling hold promise for NP treatment. In this study, through network pharmacology, molecular docking, and experimental validation, we identified the TLR4/TNF-α signaling pathway as the key molecular hub for LFS

Tab.2 Top 10 active ingredients in LFS and the topological parameters

ID	Name	Degree	DL	Source
MOL000098	Quercetin	26	0.28	multiDrug
MOL000511	Ursolic acid	17	0.75	multiDrug
MOL000006	Luteolin	12	0.25	multiDrug
MOL011865	Rosmarinic	9	0.35	multiDrug
MOL000422	Kaempferol	9	0.24	multiDrug
MOL000008	Apigenin	9	0.21	multiDrug
MOL002714	Baicalein	8	0.21	multiDrug
MOL001439	Arachidonic acid	8	0.20	multiDrug
MOL000472	Emodin	8	0.24	jigucao
MOL013179	Fisetin	7	0.24	qishugen

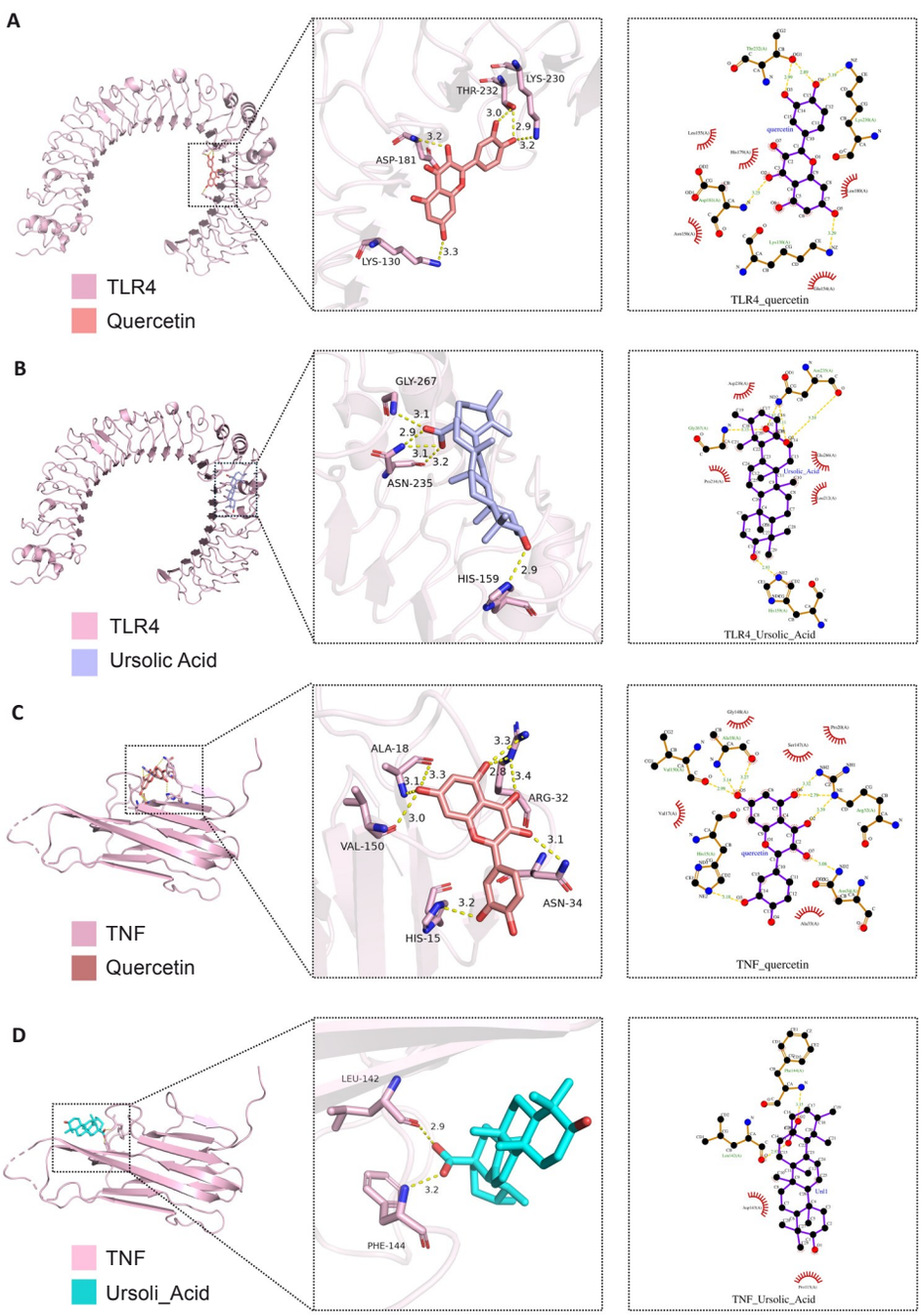

Fig. 3 Molecular docking validates TLR4/TNF-α interactions with LFS components. **A, B**: Docking results of TLR4 with quercetin and ursolic acid. **C, D**: Docking results of TNF-α with quercetin and ursolic acid.

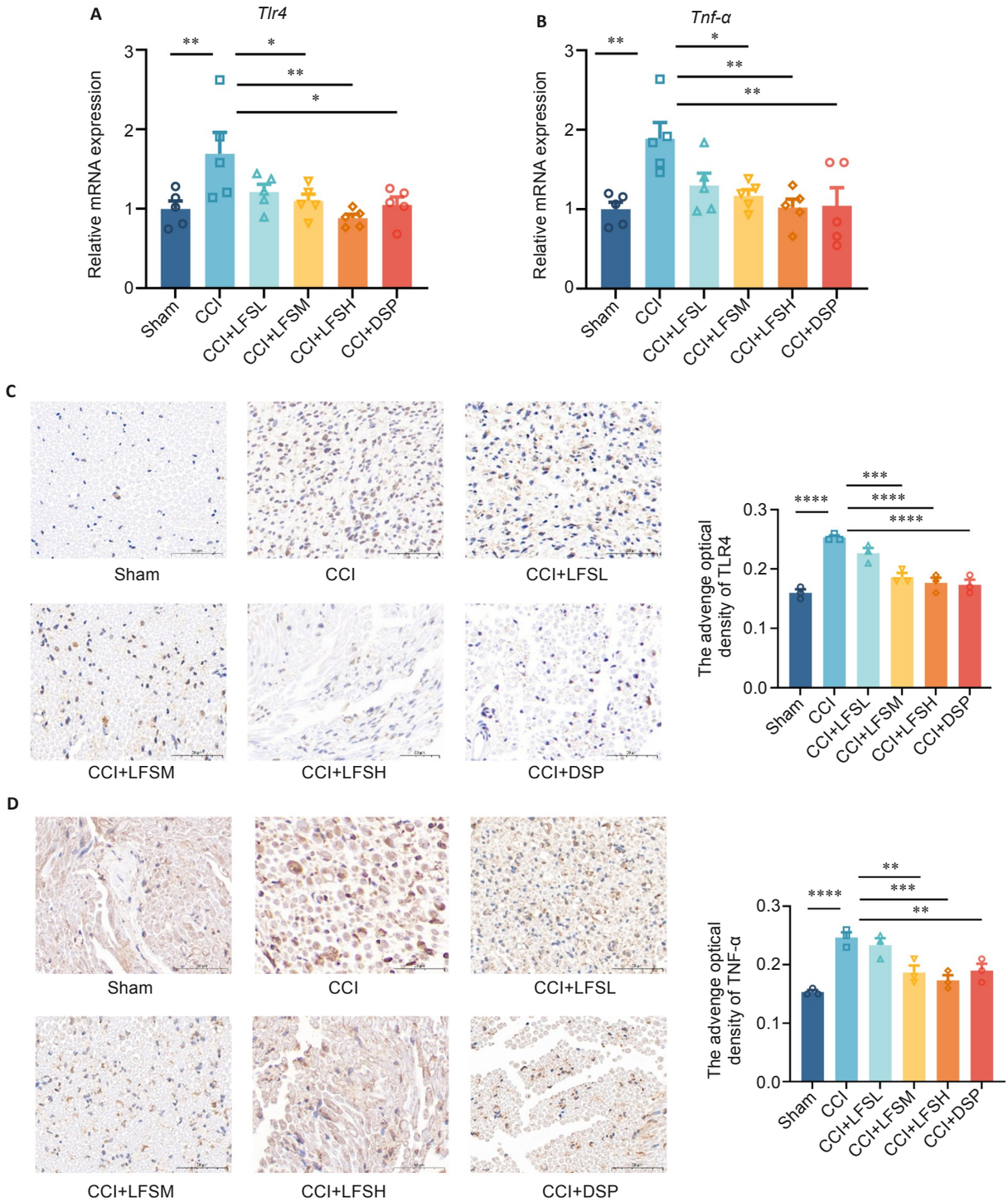

Fig.4 LFS suppress TLR4/TNF-α signaling in the spinal cord and sciatic nerve. **A**, **B**: mRNA expression of *Tlr4* and *Tnf-α* in the spinal cord (n=5). **C**, **D**: Protein expression of TLR4 and TNF-α in the sciatic nerve of mice by immunohistochemical staining (n=3). Data are presented as *Mean±SE*. *P<0.05, **P<0.01, ***P<0.001, ****P<0.0001.

against NP. KEGG analysis showed enrichment of the intersection targets of LFS for NP treatment in the TLR and TNF signaling pathways, which is consistent with previous studies showing that either the genetic knockout of *Tlr4* or pharmacological blockade of TNF-α could attenuate pain behaviors[26,27]. Importantly, LFS significantly downregulated the mRNA and protein expression of TLR4 and TNF-α in the spinal cord and sciatic nerve, and reduced inflammatory cell infiltration in the sciatic nerve, directly proving its role in blocking both peripheral sensitization (*via* TLR4) and central neuroinflammation (*via* TNF-α). This dual modulation may explain LFS's superior efficacy to the single-target therapies.

When screening active components of LFS, quercetin (DL=0.28) and ursolic acid (DL=0.75) satisfied the standards for drug-likeness (DL>0.18) and were the top 2 bioactive components of LFS. Both

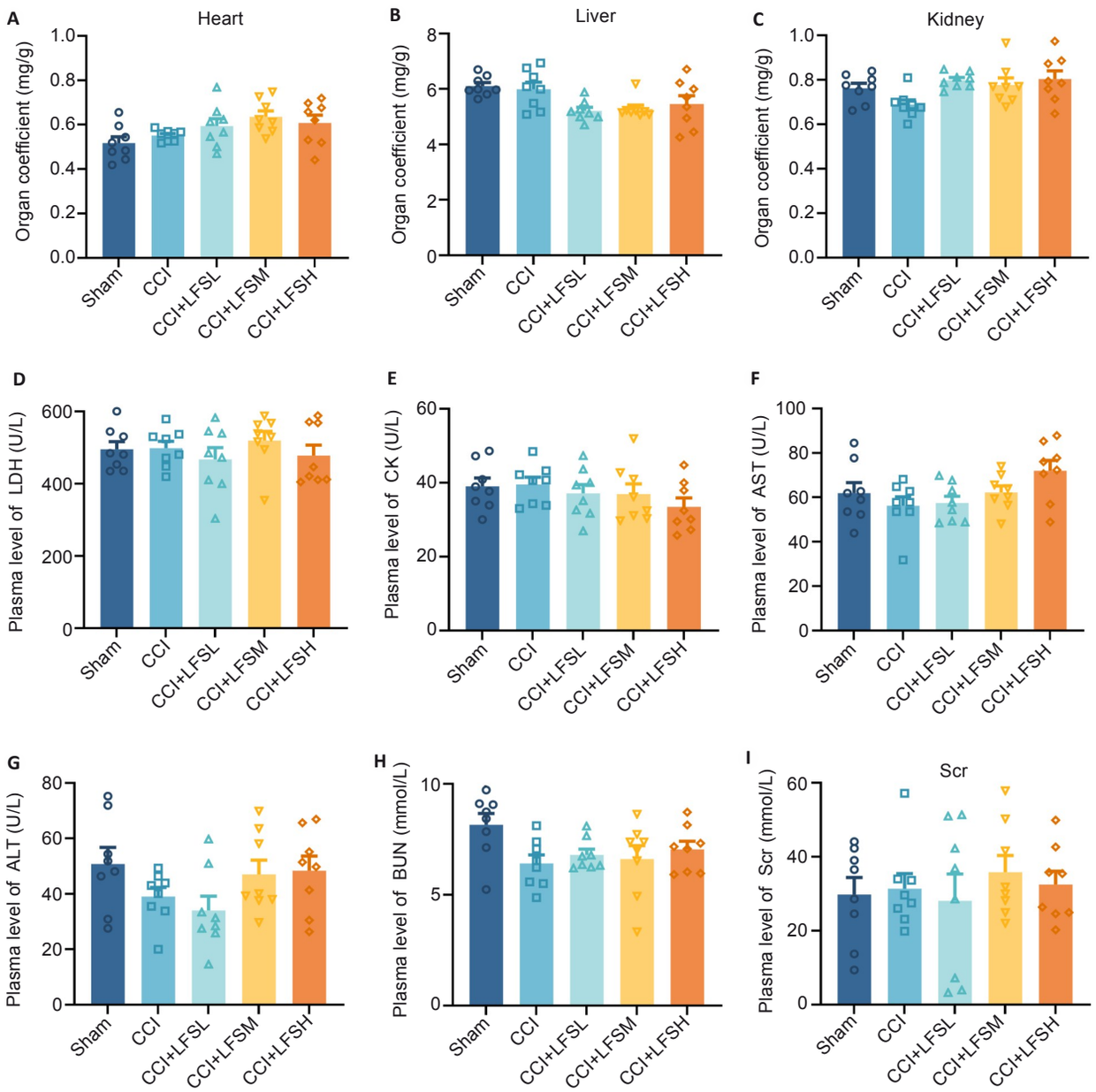

Fig. 5 Biosafety of LFS in the treatment of NP. **A-C**: Organ index of the heart, liver, and kidneys (n=8). **D-I**: Plasma levels of LDH, CK, AST, ALT, BUN and Scr in mice (n=8). Data are presented as *Mean±SE*.

quercetin and ursolic acid were directly associated with the hub genes (e.g., TNF) in the PPI network (Fig. 2B-D). Emerging evidence confirms the anti-nociceptive efficacy of quercetin in rodent models of inflammatory, neuropathic, and cancer pain, while ursolic acid exhibits potent anti-inflammatory and antioxidant activities to alleviate CCI-induced neuropathic behaviors[28, 29]. Critically, quercetin serves as a primary bioactive compound in *Angelica sinensis*, *Carthamus tinctorius* and *Panax notoginseng*, whereas ursolic acid is enriched in *Schizonepeta tenuifolia* and *Panax notoginseng*, all of which are essential constituents of in the formula of LFS[30-34]. Quercetin and ursolic acid exhibit the highest degree values in the compound-target network, indicating their roles as the most pivotal components connecting the greatest number of targets and acting at the core junctures of the entire disease network. Furthermore, multiple studies have demonstrated that quercetin and ursolic acid exert anti-inflammatory and analgesic effects to alleviate neuropathic pain through transdermal or topical administration[35, 36]. Quercetin has been shown to effectively address various skin issues, including acne, inflammation, wounds, and cancer. Ursolic acid possesses transdermal potential for the treatment of arthritis[37, 38]. Molecular docking further revealed high-affinity binding of these compounds to TLR4 (quercetin: -6.9 kcal/mol; ursolic acid: -6.3 kcal/mol) and TNF-α (quercetin: -7.1 kcal/mol; ursolic acid: -7.3 kcal/mol), providing structural validation for their anti-inflammatory mechanisms. This bridges the empirical use of TCM with modern pharmacology, illustrating how herbal synergies can target complex signaling networks.

The clinical dosage regimen of LFS involves

transdermal application of one patch (8.8 cm×10 cm each) daily on the affected area. To align with clinical practice, doses were translated using body surface area (BSA) normalization, a gold standard for interspecies scaling[39]. Using the standard conversion factor of 0.025 for human-to-mouse BSA equivalence (human BSA= 1.6 m^2, mouse BSA=0.04 m^2), the equivalent mouse dose was calculated as: clinical dose per patient (cm^2) × conversion factor=8.8×10×0.025=4.4 cm^2. Experimental doses 2.2, 4.4 and 8.8 cm^2 thus represent 50%, 100%, and 200% of the clinical equivalence[40-42]. The CCI model was selected for its translational relevance, as it recapitulates human NP features, including mixed inflammatory-neurogenic pain and spontaneous neuronal hyperexcitability, ensuring the biological plausibility of our findings.

In conclusion, this study systematically demonstrates that LFS effectively alleviates NP in a CCI mouse model *via* dose-dependent suppression of TLR4/TNF-α-mediated neuroinflammation, while maintaining an good biosafety profile with no observed organ toxicity. These findings validate LFS as a promising transdermal therapeutic alternative for NP management, providing a scientific basis for the application of traditional Chinese medicine compounds and shedding light on novel strategies targeting the neuroinflammatory pathways in pain therapy.

Declaration of interests: The authors declare no competing interests.

REFERENCES:

[1] Attal N, Bouhassira D, Colvin L. Advances and challenges in neuropathic pain: a narrative review and future directions [J]. Br J Anaesth, 2023, 131(1): 79-92.

[2] Cohen SP, Mao J. Neuropathic pain: mechanisms and their clinical implications [J]. BMJ, 2014, 348: f7656.

[3] Ahmadi R, Kuner R, Weidner N, et al. The Diagnosis and treatment of neuropathic pain [J]. Dtsch Arztebl Int, 2024, 121(25): 825-32.

[4] Ji RR, Chamessian A, Zhang YQ. Pain regulation by non-neuronal cells and inflammation [J]. Science, 2016, 354(6312): 572-7.

[5] Bannister K, Sachau J, Baron R, et al. Neuropathic pain: mechanism-based therapeutics [J]. Annu Rev Pharmacol Toxicol, 2020, 60: 257-74.

[6] Si W, Li X, Jing B, et al. Stigmasterol regulates microglial M1/M2 polarization via the TLR4/NF-κB pathway to alleviate neuropathic pain [J]. Phytother Res, 2024, 38(1): 265-79.

[7] Qindeel M, Ullah MH, Fakhar UD, et al. Recent trends, challenges and future outlook of transdermal drug delivery systems for rheumatoid arthritis therapy [J]. J Control Release, 2020, 327: 595-615.

[8] Wu TF, Deng J, Wang X, et al. Textual research on Bungarus Parvus [J]. Chin J Chin Mater Med, 2023, 48(22): 6234-48.

[9] Chawla R, Kumar S, Sharma A. The genus Clematis (Ranunculaceae): chemical and pharmacological perspectives [J]. J Ethnopharmacol, 2012, 143(1): 116-50.

[10] Wang LL, Kang ML, Liu CW, et al. Panax notoginseng saponins activate nuclear factor erythroid 2-related factor 2 to inhibit ferroptosis and attenuate inflammatory injury in cerebral ischemia-reperfusion [J]. Am J Chin Med, 2024, 52(3): 821-39.

[11] Chen Y, Duan JA, Qian D, et al. Assessment and comparison of immunoregulatory activity of four hydrosoluble fractions of Angelica sinensis *in vitro* on the peritoneal macrophages in ICR mice [J]. Int Immunopharmacol, 2010, 10(4): 422-30.

[12] Zhao WH. The clinical effect observation of luofushan rheumatism plaster intreatment of sciatica [J]. Chin J Clin Rational Drug Use, 2018, 11(19): 30-31.

[13] AL HANBALI O A, KHAN HMS, Sarfraz M, et al. Transdermal patches: design and current approaches to painless drug delivery [J]. Acta Pharm, 2019, 69(2): 197-215.

[14] Borgonetti V, Governa P, Biagi M, et al. *Zingiber officinale* Roscoe rhizome extract alleviates neuropathic pain by inhibiting neuroinflammation in mice [J]. Phytomedicine, 2020, 78: 153307.

[15] Feng X, Ju P, Chen Y, et al. Analgesic alkaloids from *Urticae Fissae* Herba [J]. Chin Herb Med, 2022, 14(1): 125-9.

[16] Ayik B, Ortadeveci A, Bakilan F, et al. Comparison of the effects of perineural and intraperitoneal ozone therapy on nerve healing in an experimental sciatic nerve injury model [J]. Medicina (Kaunas), 2024, 60(12): 2097

[17] Zhou Y, Zhou B, Pache L, et al. Metascape provides a biologist-oriented resource for the analysis of systems-level datasets [J]. Nat Commun, 2019, 10(1): 1523.

[18] Wang ZY, Han QQ, Deng MY, et al. Lemairamin, isolated from the Zanthoxylum plants, alleviates pain hypersensitivity via spinal α7 nicotinic acetylcholine receptors [J]. Biochem Biophys Res Commun, 2020, 525(4): 1087-94.

[19] Kumar N, Goel R, Ansari MN, et al. Formulation of phytosomes containing *Rubia cordifolia* extract for neuropathic pain: in vitro and *in vivo* evaluation [J]. ACS Omega, 2024, 9(23): 25381-9.

[20] Li L, Sun L, Qiu Y, et al. Protective effect of stachydrine against cerebral ischemia-reperfusion injury by reducing inflammation and apoptosis through P65 and JAK2/STAT3 signaling pathway [J]. Front Pharmacol, 2020, 11: 64.

[21] Tanimura Y, Yoshida M, Ishiuchi K, et al. Neoline is the active ingredient of processed aconite root against murine peripheral neuropathic pain model, and its pharmacokinetics in rats [J]. J Ethnopharmacol, 2019, 241: 111859.

[22] Liu M, Qiang QH, Ling Q, et al. Effects of *Danggui Sini* decoction on neuropathic pain: experimental studies and clinical pharmacological significance of inhibiting glial activation and proinflammatory cytokines in the spinal cord [J]. Int J Clin Pharmacol Ther, 2017, 55 (5): 453-64.

[23] Shoaib RM, Ahsan MZ, Akhtar U, et al. Ginsenoside Rb1, a principal effective ingredient of *Panax notoginseng*, produces pain antihypersensitivity by spinal microglial dynorphin A expression [J]. Neurosci Res, 2023, 188: 75-87.

[24] Mustafa S, Evans S, Barry B, et al. Toll-Like Receptor 4 in pain: bridging molecules-to-cells-to-systems [J]. Handb Exp Pharmacol, 2022, 276: 239-73.

[25] Mengge S, Quan J, Juan J, et al. A multicenter randomized double-blind controlled clinical study of *Luofushan* rheumatism Plaster in the treatment of rheumatoid arthritis carpal arthritis [J]. J Beijing Univ Chin Med, 2023, 46(10): 1431-42.

[26] Tange FY, Nutile-Mcmenemy N, Deleo JA. The CNS role of Toll-like receptor 4 in innate neuroimmunity and painful neuropathy [J]. Proc Natl Acad Sci U S A, 2005, 102(16): 5856-61.

[27] Svensson CI, Sshäfers M, Jones TL, et al. Spinal blockade of TNF blocks spinal nerve ligation-induced increases in spinal P-p38 [J]. Neurosci Lett, 2005, 379(3): 209-13.

[28] Liu C, Liu DQ, Tian YK, et al. The emerging role of quercetin in the treatment of chronic pain [J]. Curr Neuropharmacol, 2022, 20(12): 2346-53.

[29] Bhat RA, Lingaraju MC, Pathak NN, et al. Effect of ursolic acid in attenuating chronic constriction injury-induced neuropathic pain in rats [J]. Fundam Clin Pharmacol, 2016, 30(6): 517-28.

[30] Wu X, Liu A, Lv X, et al. Network pharmacology and experimental study of *Angelica sinensis* and *Astragalus membranaceus* capsules in treating heart failure [J]. Heliyon, 2024, 10(20): e38851.

[31] Wang W, Yang C, Xia J, et al. Novel insights into the role of quercetin and kaempferol from *Carthamus tinctorius* L. in the management of nonalcoholic fatty liver disease via NR1H4-mediated pathways [J]. Int Immunopharmacol, 2024, 143(Pt 1): 113035.

[32] Han J, Hou J, Liu Y, et al. Using network pharmacology to explore the mechanism of *Panax notoginseng* in the treatment of myocardial fibrosis [J]. J Diabetes Res, 2022, 2022: 8895950.

[33] Zhang L, Feng Y, Ding A. The research on the chemical components of *Schizonepeta tenuifolia* Briq [J]. Chin Tradit Herb Drugs, 2001, 24 (3): 183-4.
[34] Hou W, Wei B, Liu HS. The Protective effect of *Panax notoginseng* mixture on hepatic ischemia/reperfusion injury in mice via regulating NR3C2, SRC, and GAPDH [J]. Front Pharmacol, 2021, 12: 756259.
[35] Bhat RA, Lingaraju MC, Pathak NN, et al. Effect of ursolic acid in attenuating chronic constriction injury-induced neuropathic pain in rats. Fundam Clin Pharmacol. 2016, 30(6):517-28.
[36] Muto N, Matsuoka Y, Arakawa K, et al, Quercetin attenuates neuropathic pain in rats with spared nerve injury [J]. Acta Med Okayama, 2018,72(5): 457-65.
[37] Okselni T, Septama AW, Juliadmi D, et al. Quercetin as a therapeutic agent for skin problems: a systematic review and meta-analysis on antioxidant effects, oxidative stress, inflammation, wound healing, hyperpigmentation, aging, and skin cancer [J]. Naunyn-Schmiedeberg's Arch Pharmacol, 2025, 398: 5011-55.
[38] Jamal M, Imam SS, Aqil M, et al. Transdermal potential and anti-arthritic efficacy of ursolic acid from niosomal gel systems [J]. Int Immunopharmacol, 2015, 29(2): 361-9.
[39] Reagan-Shaw S, Nihal M, Ahmad N. Dose translation from animal to human studies revisited [J]. FASEB J, 2008, 22(3): 659-61.
[40] Gopalsamy B, Sambasevam Y, Zulazmi NA, et al. Experimental characterization of the chronic constriction injury-induced neuropathic pain model in mice [J]. Neurochem Res, 2019, 44(9): 2123-38.
[41] Starowicz K, Przewlocka B. Modulation of neuropathic-pain-related behaviour by the spinal endocannabinoid/endovanilloid system [J]. Philos Trans R Soc Lond B Biol Sci, 2012, 367(1607): 3286-99.
[42] Colleoni M, Sacerdote P. Murine models of human neuropathic pain [J]. Biochim Biophys Acta, 2010, 1802(10): 924-33.

罗浮山风湿膏药通过抑制TLR4/TNF-α信号通路缓解小鼠神经病理性疼痛

傅玉芳[1],谭伟玲[1,2],李小翠[1],林荣钿[3],刘叔文[1,4,5],叶 玲[1,5]
南方医科大学[1]药学院,[2]中医药学院,广东 广州 510515;[3]广东罗浮山国药股份有限公司工程实验室(抗风湿中药),广东 惠州 516100;[4]南方医科大学附属坪山医院药学部,广东 深圳 518100;[5]广东省中西医结合防治情志病基础研究卓越中心,广东 广州 510515

摘要:目的 探究罗浮山风湿膏药(LFS)对神经病理性疼痛(NP)的治疗效果与作用机制。**方法** 构建坐骨神经慢性压迫性损伤(CCI)小鼠模型,分别以低、中、高剂量(2.2、4.4、8.8 cm²)的LFS连续干预14 d。通过检测机械刺激缩足反射阈值(MWT)和热刺激缩足反射潜伏期(PWL),血浆炎症因子IL-6、TNF-α水平,以及坐骨神经组织病理学分析评估其治疗效果;采用网络药理学与分子对接技术筛选LFS抗NP的关键靶点及通路;通过RT-qPCR和免疫组化验证相关靶点和通路;最后测定心脏、肝脏、肾脏脏器系数及功能损伤标志物评价安全性。**结果** 与CCI模型组相比,LFS可剂量依赖性地升高MWT与PWL,降低血浆炎症因子IL-6、TNF-α水平,减轻坐骨神经炎症的损伤程度($P<0.05$)。网络药理学分析显示,LFS含378种活性成分,可作用于279个NP相关基因,主要富集于TLR和TNF信号通路。分子对接结果表明,LFS关键成分槲皮素和熊果酸可与TLR4和TNF-α靶点稳定结合。与CCI模型组相比,LFS可剂量依赖性地下调脊髓组织中*Tlr4*和*Tnf-α*的mRNA表达水平,小鼠坐骨神经中TLR4和TNF-α蛋白的表达亦同步降低($P<0.05$)。安全性评估显示,各剂量LFS组脏器系数及心肝肾损伤标志物与CCI组和假手术组差异无统计学意义($P>0.05$)。**结论** LFS通过抑制TLR4/TNF-α通路介导的神经炎症缓解NP,且具有良好的安全性。

关键词:罗浮山风湿膏药;神经病理性疼痛;TLR4/TNF-α通路;安全性评价

收稿日期:2025-08-03

基金项目:基于临床导向的罗浮山风湿膏功效科学内涵研究(K924319081);国家自然科学基金(82422077);广东省自然科学基金(2024B1515020093)

作者简介:傅玉芳,在读硕士研究生,E-mail:fyf2001021600@163.com

通信作者:叶 玲,博士,教授,E-mail:yeling@smu.edu.cn;刘叔文,博士,教授,E-mail:liusw@smu.edu.cn;林荣钿,本科,E-mail: 47415242@qq.com